Supplementary information

(1) Phase transformation for (6,0) CNT toward (6,0)-hA or hP24 carbon

For comparison, the pathways from (6,0)-CNT toward hP24 and (6,0)-hA are also simulated at 0, 5, 10, and 15 GPa. The pathways are given in Fig. S1(a) and Fig. S1(b), respectively. As shown in Fig. S1(a), hP24 can be formed from (6,0)-CNT via a three-fold distortion assisted intertube bonding mechanism around the hexagonal corners, where the center of CNT is located at the (1/3, 2/3, z) position. Meanwhile, as shown in Fig. S1(b), polymerized (6,0)-hA phase can be formed from (6,0)-CNT via a six-fold distortion assisted intertube bonding mechanism around the hexagonal centers, where the center of CNT is located at the (0.5, 0.5, z) position. The enthalpy along the pathways toward the formation of (6,0)-hP24 and (6,0)-hA are plotted in Fig. S1(c). We can see that (6,0) CNT can easily convert to hP24 phase with a relatively small barrier of 0.084, 0.030, 0.009, and 0.004 eV/atom at 0, 5, 10, and 15 GPa, respectively. Moreover, the hP24 structure is always more stable than (6,0)-hA and (6,0) CNT. Thus, (6,0) CNT can be more easily converted to hP24 than (6,0)-hA from both the kinetic and energetic points of view. Throughout the phase transformation from (6,0)-CNT toward (6,0)-hP24 under 5 GPa, the lattice parameters *a*, *b*, and *c* are about -10.60% -10.60%, and -1.13% compressed, respectively, showing a strong in-plane direction-dependent pressure response, as well as the phase transformation from (9,0)-CNT toward (9,0)-hP36 phase shown in Fig. 3.

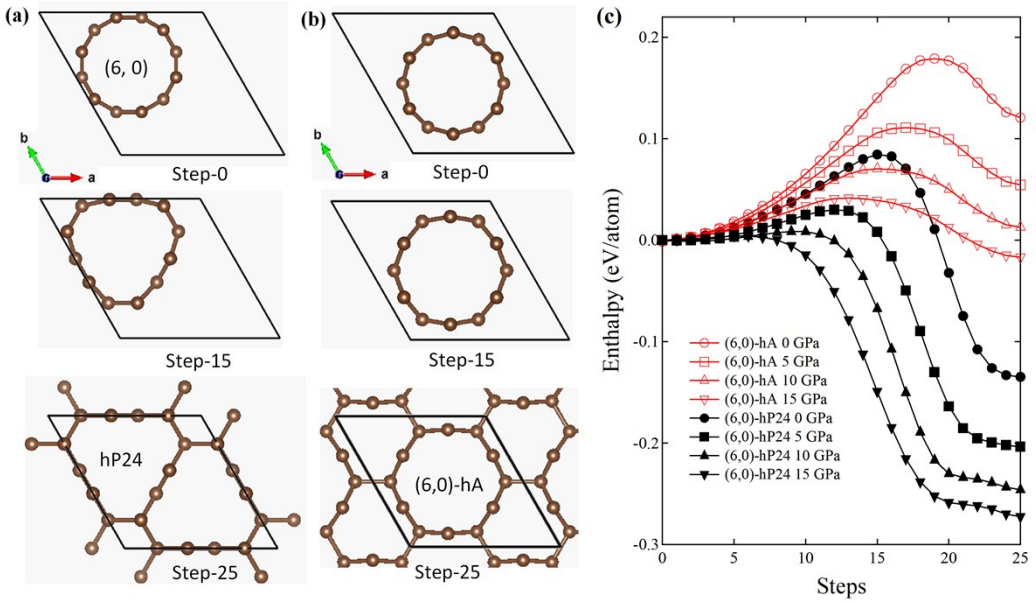

Fig. S1: (a) Structural snapshots along the pathway from (6,0)-CNT toward (6,0)-hP24 via a three-fold distortion assisted intertube bonding mechanism around the hexagonal corners, where the center of CNT is located at the (1/3, 2/3, z) position; (b) Structural snapshots along the pathway from (6,0)-CNT toward (6,0)-hA via a six-fold distortion assisted intertube

bonding mechanism around the hexagonal centers, where the center of CNT is located at the (0.5, 0.5, z) position. (c) Enthalpy versus pathways for the transformation from (6,0)-CNT toward hP24 and (6,0)-hA structure at 0, 5, 10, and 15 GPa.

(2) Calculated energy for (6,0)-C, (9,0)-C, and (12,0)-hP48

For comparison, we have also calculated the total energy as a function of volume for (6,0)-C (*I4/mcm*) derived from (6,0)-CNT and orthorhombic (9,0)-C (*Cmcm*) derived from (9,0)-CNT reported by Lian *et al.*[1] with a tetragonal or orthorhombic initial configuration of CNTs. One can see that the tetragonal (6,0)-C and orthorhombic (9,0)-C have a relative larger volume, but less stable compared to (6,0)-hP24 and (9,0)-hP36 with an energy loss of 0.082 and 0.043 eV per atom, respectively. Moreover, we also calculated the total energy as a function of volume for (12,0)-CNT and the derived (12,0)-hP48 carbon. The calculated total energy is -8.962 eV/atom for (12,0)-hP48 carbon, which is comparable to -8.967 eV/atom for the corresponding (12,0)-CNT. For comparison, the energy for (3,0)-hP12 (*i.e.* hexagonal diamond, HD) is also added in Fig. S2. We can see that hP12 is less stable than cubic diamond and graphite, but more stable than hP24, hP36 and hP48 carbon.

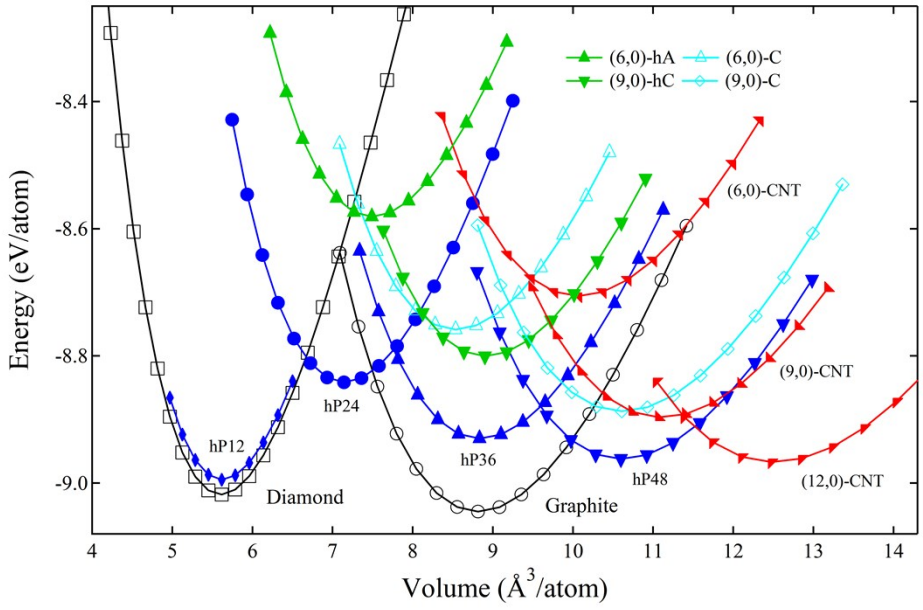

Fig. S2: Energy *versus* volume per atom for various carbon structures including (3,0)-hP12, (6,0)-C, (9,0)-C, (12,0)-CNT and (12,0)-hP48 carbon.

(3) Simulated current-voltage curves for hP24

In order to understand the transport behavior, we have simulated current-voltage curves of hP24, based on the Density-Functional Tight Binding (DFTB) method in combination with the nonequilibrium Green's function formalism.[2] The used device structures

with two semi-infinite electrodes are given in Fig. S3(a) for (6,0)-CNT, (6,0)-hP24+z (along the z-direction), and (6,0)-hP24+x (along the x-direction). The simulated current-voltage curves are plotted in Fig. S3(b). The simulated current-voltage curve for (6,0)-CNT is very closing to the recent reported data for (6,2)-CNT.[3] For (6,0)-hP24, the current data along the *z*-direction are smaller than that for (6,0)-CNT，which can be attributed to the sp^2-bonds where half carbon atoms are changed from sp^2- to sp^3-bonds in hP24. On the other hand, along the *x*-direction in hP24, the simulated current is ~ zero (10^{-13} ~ 10^{-7} mA) in the voltage range [-2, 2] duo to the sp^3-bonds along the *x*-direction. These transport properties show a similar anisotropic behavior as well as the finding in hP36 related to the effective masses.

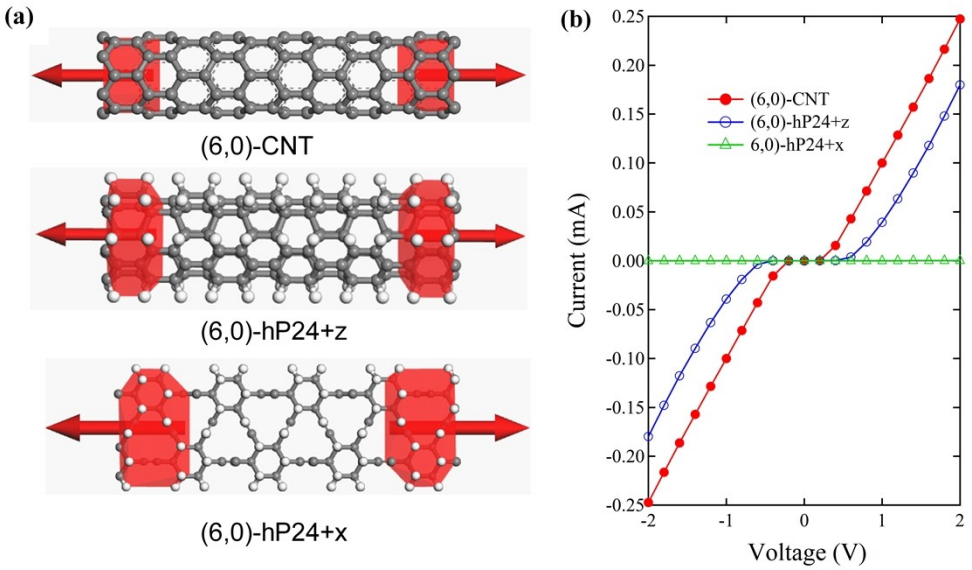

Fig. S3: (a) Device structures with two semi-infinite electrodes for (6,0)-CNT, (6,0)-hP24+*z* (along the *z*-direction) and (6,0)-hP24+*x* (along the *x*-direction). The hydrogen atoms are added to saturate the sp^3 carbon bonds in (6,0)-hP24 wire. (b) The simulated current-voltage curves for (6,0)-CNT, (6,0)-hP24+*z*, and (6,0)-hP24+*x*.

(4) Crystalline structure and electronic band structures for hP48

Beside hP24 and hP36 network structures, we have also studied the structural stability and electronic properties for hP48 carbon, derived from (12,0)-CNT. As shown in Fig. S4(a), it has a 48-atom hexagonal unit cell with lattice parameters a = 11.773 Å and c = 4.2384 Å, occupying the $12k_1$ (0.0, 0.8753, 0.0646), $12k_2$ (0.2404, 0.0, 0.0863), $12k_3$ (0.3432, 0.0, 0.9187), and $12k_4$ (0.4474, 0.0, 0.0834) Wyckoff position denoted by C_1, C_2, C_3, and C_4, respectively. The C_1 atoms form a sp^3 HD building block, while the other atoms form graphene nanoribbon, as well as in hP36. The calculated total energy is -8.962 eV/atom, which comparable to -8.967 eV/atom for the corresponding (12,0)-CNT (see Fig. S2). The

calculated phonon band structures are plotted in Fig. S4(b). No imaginary frequencies were observed throughout the entire phonon band structures, thus confirming the dynamic stability of hP48 carbon. The calculated electronic band structures under HSE06 method are given in Fig. S3(c). The conduction band minimum and valence band maximum are located at Γ point, showing a semiconductor with a direct band gap of 1.05 eV.

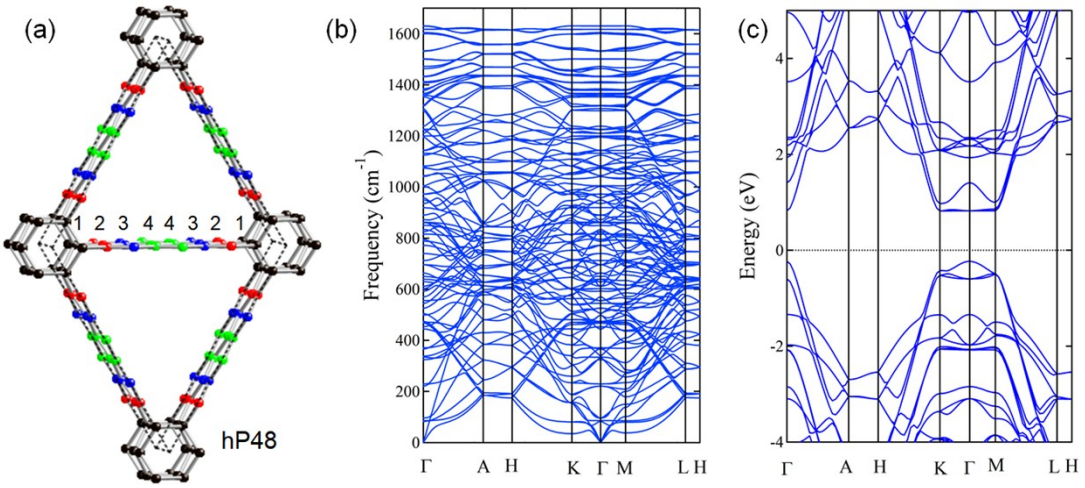

Fig. S4: (a) Network structure of hP48 derived from (12,0)-CNT; (b) Phonon band structures of hP48; (c) Electronic band structures of hP48 carbon under HSE06 method.

References

[1] C. S. Lian and J. T. Wang, *J. Chem. Phys.* 2014, **140**, 204709.

[2] A. Di Carlo, M. Gheorghe, P. Lugli, M. Stenberg, G. Seifert and Th. Frauenheim, *Physica B*, 2002, **314**, 86.

[3] M. A. Jafari, A. A. Kordbacheh, S. Mahdian and N. Ghasemi, *Physica E*, 2020, **117,** 113855.